Experimental Techniques for Mass Measurement Far From Stability

Nigel Orr,
Laboratoire de Physique Corpusculaire,
IN2P3 - CNRS, ISMRA et Université de Caen,
14050 Caen Cedex, France

Resumé

Les mesures de masse des noyaux sont un outil fondamental pour la structure nucléaire loin de la stabilité. Une revué des techniques utilisées pour ces mesures est presentée.

Abstract

The measurement of nuclear masses is a fundamental tool to probe nuclear structure far from stability. A review of the techniques that have been most commonly employed to undertake such measurements is presented.

I Introduction

Nuclear masses are directly related to the binding energies and as such reflect many of the facets of nuclear structure. General trends in binding energies may be considered as a manifestation of the global properties of nuclear matter which can be described in a first approximation in terms of a liquid drop. Superimposed on this smooth behaviour are rapid changes which reflect the microscopic structure of the nucleus – the most prominent of which are shell closures. Other effects, such as deformation may also influence the binding energy. The onset of such behaviour is often determined by adding a single nucleon. Rapid changes in the behaviour of the nuclear mass surface can thus provide a signal of such effects[1].

The ability of mass measurements far from stability to uncover structural effects is well illustrated by the now classic example provided by the breakdown in the N=20 shell closure for the neutron-rich Ne, Na and Mg isotopes. This effect was first observed through mass determinations for ^{31,32}Na [1] and ^{31,32}Mg [2] and more recently explored on a broader front by direct measurements in which some ten's of nuclei were measured in a single experiment [3, 4] (figure 1). The overbinding of the N=20-22 isotopes of Ne, Na and

[1]The nuclear mass surface is most commonly mapped through the two-neutron separation energies (S_{2n}), thus avoiding the odd-even staggering effects that arise from pairing.

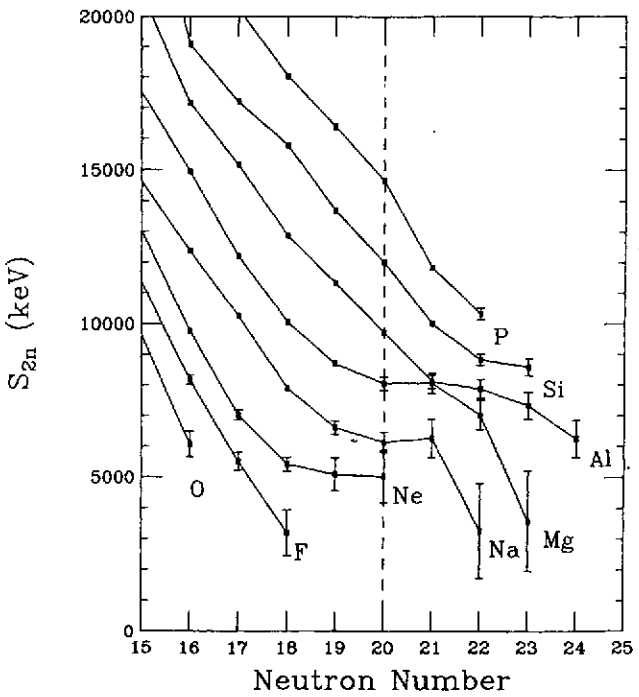

Figure 1: Two-neutron separation energies in the region of N=20 [3].

Mg has been interpreted in terms of the so-called "island of inversion" whereby prolate deformed intruder fp-shell configurations dominate the ground states [5, 6].

It is worthwhile noting that quite apart from being a fundamental quantity mass determinations represent one of the first measurements that can be undertaken of a nucleus. Indeed, many of the techniques currently employed may provide, with rates as low as a count per hour, final mass determinations with uncertainties below 1 MeV – a precision from which the gross characteristics of the nuclear mass surface may be deduced. It is clear then that mass measurements provide a means for locating the regions in which new structural effects occur, thus allowing more detailed examination employing dedicated probes to be undertaken. Again the neutron-rich N≈20 nuclei provide an example whereby the mass measurements have been followed up by detailed decay [7] and Coulomb excitation studies [8].

Beyond direct nuclear structure applications, masses far from stability are of interest as input into other fields. As discussed at length in other lectures at this school, nuclear masses are needed in the modelling of various processes in nucleosynthesis. In general, explosive processes such as the r-process are believed to proceed along pathways very far from stability (as discussed in the course of Stéphane Goriely). In such cases it may be that the majority of the nuclei involved can not yet be produced. The determination and improvement in the precisions of masses closer to stability do, however, allow the mass models used to extrapolate to the unknown masses to be refined.

Before proceeding any further a few words relating to the general challenge facing mass measurements far from stability are in order. The mass of an A=50 nucleus is of order 50 GeV. A final uncertainty of ~100 keV in the mass determination thus represents a precision of some 2×10^{-6} in the measurement. Near stability, such a precision is relatively

easily obtained. Far from stability, however, where yields are low, lifetimes short (typically less than 1 s) and reference masses scarce, attaining such precisions represents an experimental tour de force. In the following sections some of the principle techniques that have been used for such measurements are briefly outlined. As the choice of technique is intimately related to the production technique employed, these are briefly discussed.

Progress in the field, including the development of new techniques, may be followed in the Atomic Masses and Fundamental Constants (AMCO) and Nuclei Far from Stability conference series, now amalgamated as Exotic Nuclei and Atomic Masses (Bernkastel-Kues, 1992 [9], Arles, 1995 [10], Michigan 1998 [11]). A recent review of the state-of-the-art may also be found in the APAC2000 conference proceedings [12]. For the more instrumental aspects the proceedings of the EMIS conferences (Electric and Magnetic Ion Separators) are an excellent source of information. The reader is also referred to the compilations of Audi and Wapstra [13, 14] and the electronically accessible resources of the Atomic Mass Data Centre at Orsay[2].

II Production of Nuclei far from Stability

A very wide range of reactions have been used for the production of nuclei far from stability for mass measurements [15]:-

- (multinucleon) transfer and charge exchange reactions.
- deep inelastic reactions.
- fusion-evaporation reactions.
- fission.
- target spallation and fragmentation.
- projectile fragmentation and fission.

As the production and associated separation techniques have been detailed extensively in a number of recent reviews [16, 17] only a few specific comments will be made here.

Beyond the cross section for the reaction in question, the target thickness, primary beam intensity and collection efficiency of the associated spectrometer dictate the final yields. In terms of reaching the nuclei the furtherest from stability the techniques of Isotope Separation On-line (ISOL) and in-flight separation are the most widely exploited.

In the case of the former, a high energy, high intensity p or light-ion beam is used to bombard a thick production target in which fission, spallation and fragmentation may occur. The production target is coupled with an ion-source and the radioactive ions released by the target are ionised and accelerated to low energies (~100 keV) and purified using electromagnetic separation techniques. The good beam quality available with such

[2]http://www-csnsm.in2p3.fr/

a method has resulted in its use with direct measurement techniques such as high resolution mass spectrometry (traps, radio-frequency spectrometers, etc). Given the high luminosities[3] involved, the intrinsic yields are high. Unfortunately the release times and relatively short halflives can dramatical reduce the final yields.

In-flight separation involves the use of a high energy, heavy-ion beam in combination with a relatively thin target. Despite the lower luminosity, this method gains considerable advantages through the characteristics of the reaction mechanism. More specifically, the reaction products from the fragmentation (or fission) of a high energy, heavy-ion beam are confined to the very forward directions with velocities very close to that of the beam. As a result the collection efficiency of the associated spectrometer or fragment separator is very high (~30-50% at very high energies). Despite the relatively poor quality of the beams produced by in-flight techniques, they are particularly well suited to direct measurement techniques (time-of-flight, storage rings, etc) in which a large number of nuclei are measured in a single experiment.

III Experimental Methods for Mass Measurements

In this section the principle methods used to measure the masses of nuclei far from stability are discussed. In general terms two distinct classes of techniques exist:

- Q-value determination – reactions or decay.
- Direct measurement – mass spectrometry, time-of-flight, cyclic/frequency measurements.

By way of a summary, Table 1 presents a resumé of the various techniques, including an estimate of the precision attainable (for a nucleus of A~50) and the principle advantages and difficulties.

1 Q-value Determinations

Mass differences and hence binding energies may be derived from the energy balance in reactions and decay processes. For example, in a two-body reaction denoted by $a(b,c)d$, the mass excesses (Δ) are related by,

$$Q = \Delta_a + \Delta_b - \Delta_c - \Delta_d \tag{1}$$

where the Q-value is the amount of energy released in the reaction. If three of the masses are well known, the determination of the Q-value from a measurement of the reaction kinematics will allow the mass of the remaining reaction partner — usually the ejectile, c, or recoil, d — to be deduced.

[3]Primary beam intensity × target thickness.

Technique	Production Method	Precision	Comments	Example
Reaction Q-value	light-ion transfer	~1-10 keV	limited ΔT_z	^{200}Pb (INS)
	heavy-ion multi-nucleon transfer	~50 keV	$\Delta T_z \leq 2$ low σ (~1μb/sr) backgrounds, g.s. id. E_x ejectile/residue unbound nuclei	^{13}Be, ^{16}B (HMI) ^{11}N (GANIL)
	pion double-charge exchange	~50-200 keV	$\Delta T_z = 2$ v. low σ (<1μb/sr) backgrounds, g.s. id. tgt material	^{14}Be (LAMPF)
Decay Q-value (β, p, α)	fusion-evaporation target spallation/frag. proj. frag., fission	~10-1000 keV	decay scheme end-point determination unbound nuclei (p, α-decay)	^{80}Zn (TRISTAN)
Invariant Mass	proj. frag.	~100-500 keV	complete kinematics unbound nuclei	^{10}He (RIKEN)
Mass Spectrometry	fusion-evaporation target spallation/frag. fission	~10-100 keV	precision V meas. source contaminates	A~100 In,Br (TASCC)
Direct TOF	proj. frag. target spallation/frag.	~100-1000 keV	many Δ's meas. many ref. Δ's v. short $t_{meas.}$ μs-isomers	N~20,28 (SPEG)
Cyclotron	fusion-evaporation [target spallation/frag. fission]	~100 keV	v. long d_{flight} low trans. (double CSS) v. short $t_{meas.}$	^{100}Sn (CSS-GANIL)
Storage Ring with cooling as a TOF spectrometer	proj. frag./fission proj. frag./fission	~10 keV [?]	cooling t~1 s very high R (isomers) low inject. eff. v. short $t_{meas.}$	A~200 Hg,Pb,Po (ESR-GSI)
Radio-Frequency Mass Spectrometry	[fusion-evaporation] target spallation/frag. [fission]	[~10 keV]	v. short $t_{meas.}$ low trans. efficiency	N~20 Z=11,12 (MISTRAL)
Trap	[fusion-evaporation] target spallation/frag. [fission]	~10 keV	cooling, trapping (t~1 s) very high R (isomers) low coll./trans. efficiency	A~190 Hg (ISOLTRAP)

Table 1: Resumé of mass measurement techniques.

Similarly, the Q-value of a decay process (β or direct particle emission) may be used to determine a mass difference. In the case of beta-decay the situation is complicated by continuous energy spectra resulting from the three-body decay channel. The energy released in the decay is, ignoring recoil effects, the maximum or so-called endpoint energy of the electron or positron.

a Transfer Reactions

Low energy (~5-30 MeV/nucleon) transfer reactions have long played an important role in measuring mass excesses. The fundamental requirement of such experiments is the measurement of an energy spectrum of one of the two reaction products (usually the beam-like ejectile). As good resolution is needed to make a precise determination of the reaction Q-value and separate the ground and any excited states in the exit channel, these studies have employed for the most part high resolution, broad range magnetic spectrographs. Importantly a spectrograph compensates for the kinematic variation in energy of the ions over the range of accepted angles and focuses the reaction products of a particular reaction according to the Q-value. The determination of the Q-value of the reaction of interest is made using a calibration derived from reactions of known Q-value.

Historically, due to the availability of the beams, light ion induced reactions were first used [18, 19]. The mainstay of studies of neutron-rich nuclei have been the (d,^{3}He) [20], (t,p) [21] and (t,^{3}He) [22] reactions. On the proton-rich side of stability the 2-, 3- and 4-neutron pickup reactions (p,t) [23], (^{3}He,^{6}He) [24] and (α,^{8}He) [25] which was first employed to determine the mass of ^{8}He [23], have proved invaluable tools, particularly when coupled to N=Z targets. Given the inherently high resolution possible with light-ion reactions, quite precise mass determinations (~1-20 keV) can be made. However, particularly for the neutron-rich nuclei, light-ion studies are usually restricted to relatively close to stability ($\Delta T_z \leq 1$) and have, with the advent of heavy-ion beams, largely fallen into disuse. The α-beam neutron pickup reactions remain notable exceptions, as recently demonstrated by the work of Kato *et al.* [26].

While suffering from poorer resolution than light ion reactions, heavy ion induced reactions can reach further from stability ($\Delta T_z \leq 2$) and still provide reasonably precise mass determinations (~20-50 keV). Reactions such as (^{7}Li,^{8}He) [27, 28] and (^{14}N,^{15}C) [27, 29] have been used to probe proton-rich nuclei, however, the emphasis has tended to be on the neutron-rich. In the latter case the use of targets and beams of the most neutron-rich stable isotopes has proved essential to reach as far as possible from stability. This is well demonstrated by the development of highly enriched targets and, to a lesser extent sufficiently intense beams, of the rare isotopes ^{34,36}S which proved crucial for measurements of nuclei in the vicinity of the N=20 shell closure [30, 31, 32, 33]. More recently, targets and beams of the long lived radionuclides ^{10}Be and ^{14}C have allowed significant advances to be made for the very light, neutron-rich nuclei [34, 35, 56] (figure 2).

Multinucleon transfer reactions present a number of specific experimental difficulties which arise for the most part from the low reaction cross sections. Owing to the the very negative Q-values, high l-transfers are prefered, often resulting in the excited states being

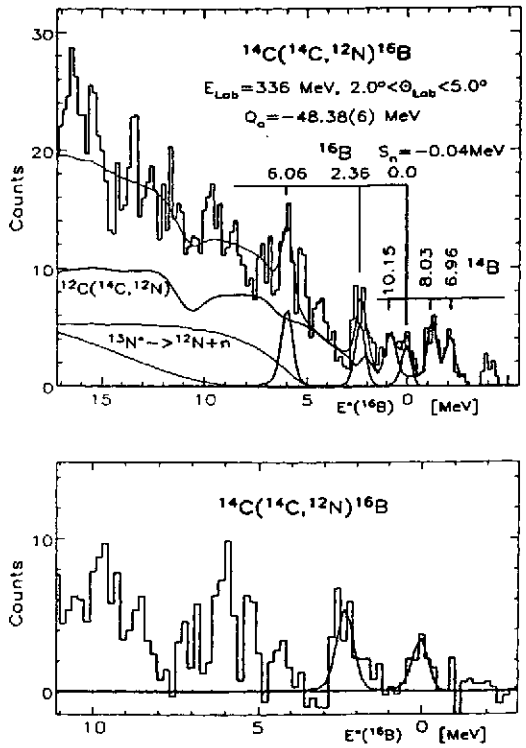

Figure 2: Top panel: Excitation energy spectrum for the reaction $^{14}C(^{14}C,^{12}N)^{16}B$ [56]. Note the background arising from reactions on the small amount of ^{12}C present in the target. Bottom panel: Same spectrum after subtraction of a spectrum taken using a ^{12}C target.

more strongly populated than the ground state. In addition, complications can also arise from the differences in selectivity of different reactions (as illustrated, for example, by the case of ^{10}Li [36, 37, 38, 39, 41, 42, 40]). Considerable care must be given, therefore, to identifying the ground state, especially in the presence of reactions on the target backing etc. Usually careful subtraction of spectra obtained for the same reaction on targets of the "contaminants" is sufficient. In some circumstances more sophisticated techniques are necessary, particularly when reactions on the contaminants are very prolific [43, 44, 45].

b Pion Double Charge Exchange (DCX)

Pion double charge reactions ($\pi^{\pm}$,$\pi^{\mp}$), with $\Delta T_z = 2$, have been employed with considerable success to measure the masses of a number of light and medium mass nuclei using the EPICS spectrometer at Los Alamos [46, 47, 48, 49, 50, 51].

$$Q = \Delta_a - \Delta_d \pm 2m_e c^2 \tag{2}$$

Experimentally the method is similar to that used for transfer reactions with the constraint that the calibration reaction is DCX as well. Moderate uncertainties in the mass determinations (~50-150 keV) have been achieved, with the principle limitation arising from the statistical quality of both the reaction and calibration data. In practice the measurements are challenging owing to the weak reaction cross sections (~100-500 nb/sr) coupled with low pion fluxes — some 10^8 pps as compared to ~10^{11-12} pps for heavy-ion beams. As very

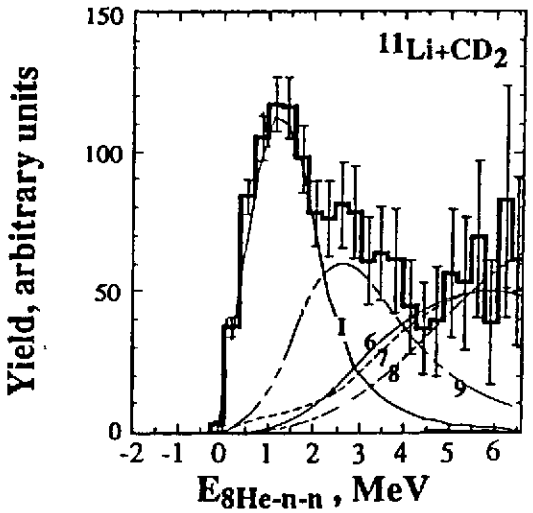

Figure 3: Invariant mass spectrum for ^{10}He produced via proton stripping from a ^{11}Li beam, as reconstructed from the decay fragments ^{8}He + 2n [57].

thick targets are used in compensation and the beam spot size is large (typically 10-20 cm) prohibitively large quantities of target material (~20-200 g) are needed. This has, with the notable exception of the measurement of the mass of ^{14}Be with a ^{14}C target [49], precluded the use of rare isotopic materials.

While reaction Q-value measurements have largely fallen out of use in recent years, due principally to the advent of direct methods, they can in specific cases still play an important role. In particular, the masses of particle unbound systems can be accessed (eg., ^{9}He [50, 53], ^{10}He [54], ^{10}Li [38, 39, 40], ^{13}Be [55] and ^{16}B [56]). Additionally, reaction Q-value mass determinations are typically superior in precision to those furnished by direct time-of-flight measurements and can, as in the case of ^{11}Li [34, 51], provide key data [52].

c *Invariant Mass Measurements*

Techniques have emerged in recent years with which light, unbound nuclei can be investigated via measurements of the in-flight decay [57, 58, 42]. The nuclei are produced using reactions with radioactive beams and from the momenta of the reaction products the decay energy or so-called invariant mass spectrum may be constructed, thus providing a measure of the mass of the system. As illustrated by the ^{10}He measurement of Korsheninnikov *et al.* [57], in which one-proton stripping from ^{11}Li beam was employed, quite large scale detector arrays are required to provide for the detection of the decay fragments (^{8}He and two neutrons). Given the quite low event rates and relatively low resolution of such measurements the final precision is considerably poorer (300 keV in the ^{10}He measurement, see figure 3 [57]) than in reaction Q-value measurements.

In a variation of the technique fragmentation of a stable beam (^{18}O) was employed to populate ^{10}Li and ^{13}Be and the relative velocities of the neutron and charged fragments (^{9}Li

and ^{12}Be) measured at zero degree [41, 42]. In both cases, the results suggested that these systems are more bound than was determined from transfer reactions [36, 38, 39, 40, 55].

Despite the relative complexity of the measurements described here they do present some specific advantages. Firstly, secondary beams allow such measurements to be extended, in principle, to much heavier systems than classical transfer or DCX experiments (although presently available beam intensities limit work to the lightest systems). Additionally, the few nucleon transfer or fragmentation reactions used to populate the systems of interest can compliment the selectivity of multi-nucleon transfer reactions.

d Decay Measurements

In principle the masses for all bound nuclei off the stability line may be determined from the measurement of the Q-value associated with the β-decay. This approach has, consequently, been employed across a wide range of nuclei in association with most production methods.

In the case of nuclei on the neutron-rich side of stability, decay is accompanied by the emission of an electron and the mass difference is simply,

$$Q_{\beta^-} = \Delta_a - \Delta_d \tag{3}$$

For proton-rich nuclei decay may occur with the emission of a positron,

$$Q_{\beta^+} = \Delta_a - \Delta_d - 2m_e c^2 \tag{4}$$

or via electron capture,

$$Q_{EC} = \Delta_a - \Delta_d \tag{5}$$

Usually the mass of the daughter *(d)* is known and the mass of the parent *(a)* may be deduced[4]. Decay may occur to either the ground or excited states of the daughter and in the latter case, the mass differences must be adjusted by the excitation energy of the state fed by the measured transition. Far from stability, however, decay schemes are often poorly known and it is necessary to measure the β-particles in coincidence with gamma rays in order to establish the decay scheme. Often then, the Q-value for the decay is derived from the feedings to a number of excited states as well as to the ground state (figure 4, [59]).

In β^--decay the Q_{β^-} is determined directly from the endpoint of the electron energy spectrum (figure 4). The electron spectra are typically measured using solid state detectors [60, 61], scintillation counters [62] or magnetic spectrometers [63], though the latter require comparitively high source activities. Given the decreasing number of events in the spectra as the endpoint energy is approached, considerable care must be exercised in making the measurements and the response function of the detector should be well understood [60]. The data treatment has consequently often employed shape fitting techniques [64] rather than the classical Fermi-Kurie plot analysis [65]. Approaches have also been developed to reduce distortions in the measurements of the electron energies [63, 62].

[4]The mass determination of ^{32}Mg [2] is an interesting exception whereby the mass of the parent, ^{32}Na, had been determined previously via direct mass spectroscopy [1])

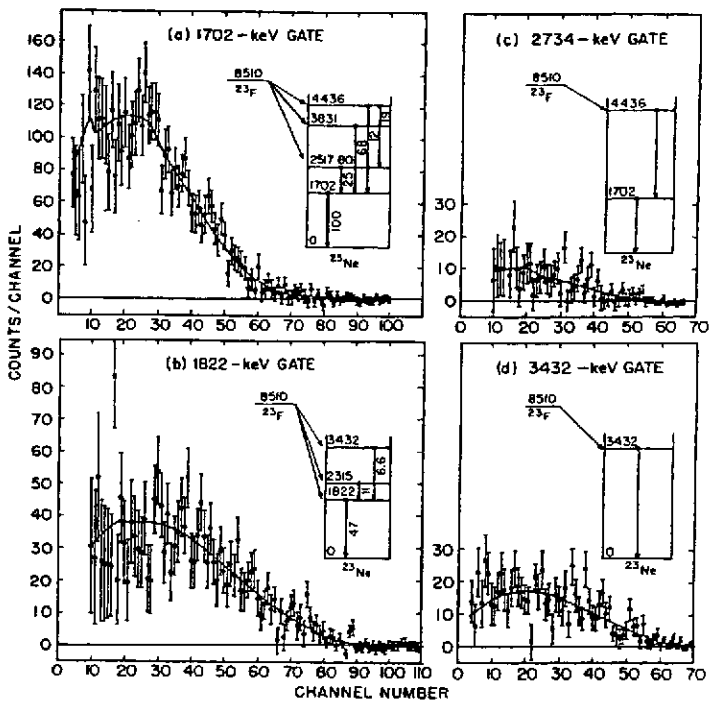

Figure 4: Beta-energy spectra from the decay of ^{23}F leading to different excited states in ^{23}Ne [59].

In β^+-decay two approaches have been employed to determine the Q_{EC}. As in the case of β^--decay, it may be obtained via a direct measurement of the endpoint of the positron energy spectrum. Such a measurement is prone, however, to distortions arising from summing of the positron energy with the annihilation radiation. An innovative approach to these problems has been made through the development of a summation-free, β^+-endpoint spectrometer [66].

A second method employs the ratio of positron emission to electron capture in the decay; more specifically the ratio $\beta^+/(\beta^+ + \mathrm{EC})$ [67]. As this ratio is strongly dependant on the endpoint energy the Q_{EC} may in principle be deduced. This method is very sensitive, however, to the feeding of high lying levels in the daughter, which are often difficult to detect. Given the difficulties presented by both methods care must be taken in interpreting the results of Q_{EC} determinations [66, 68].

Given the need to undertake coincidence measurements and establish the endpoint energy from a continuous spectrum, β-decay Q-value mass determinations are limited by the production rates. Nevertheless in some cases, such as neutron-rich fission products [69], β-decay measurements still represent the most viable approach. Apart from systematic errors that may result from incomplete knowledege of the decay scheme, precisions from $\sim$10 keV to 1 MeV may be obtained depending on the statistical quality of the data.

Measurements of direct particle (proton or α) decay can also provide mass differences and the masses of nuclei beyond the drip-line may be accessed in this manner. Given that the lifetime must be sufficiently long that the decay can be observed, such measurements are restricted to nuclei above A$\simeq$100. As the decay energies are discrete quite high precisions ($\sim$10 keV) are attainable. The accuracy of such measurements may be comprimised,

however, by the decay or feeding of a level which is not the ground state. For example, in α-decay, while the strongest branch in the decay of even-even nuclei is that to ground state of the daughter, it is not in general the case for odd-odd or odd-even nuclides [13]. In addition, often neither the mass of the parent or daughter is known.

Given then the large quantity of data accumulated on α-decay chains [14], such systematics offer a potentially rich source of information if the mass of one of the members can be determined. Such has been the case, for example, in recent measurements of the (α,^{8}He) reaction [26].

2 Direct measurements at low energy

All direct mass measurement techniques operate according to the same basic principle, namely that the magnetic rigidity ($B\rho$) is related to the time-of-flight (TOF) through the system in question, or the cyclotron frequency (ω),

$$\frac{B\rho}{v} = \gamma\frac{m}{q} = \frac{B}{\omega} \tag{6}$$

where v is the ion velocity, m is the mass, q is the charge state and γ is the Lorentz factor. In principle all the variables can be measured absolutely. However, in order to increase the precision to that needed to provide a meaningful mass determination, the measurements are made with respect to well known reference masses.

a High Resolution mass spectrometers

Mass spectrometers operate according to the simple principle whereby if two ions of mass M_A and M_B are accelerated under potentials V_A and V_B, follow identical trajectories (as defined by the entrance and exit slits) while being subject to the same static magnetic field then,

$$\frac{M_A}{M_B} = \frac{V_B}{V_A} \tag{7}$$

The mass determination thus relies on an accurate measurement of the potentials V_A and V_B.

The first direct mass measurements of short lived isotopes, including the neutron-rich Na isotopes, were performed in the mid 1970's at ISOLDE,CERN using a single stage mass spectrometer with a resolving power of $R = M/\Delta M$=650 [1]. Owing to the characteristics of the surface ionization ion-source and the need for relatively high intensity beams only the alkali elements could be studied.

In subsequent experiments the masses of neutron deficient and rich isotopes of rubidium ($^{74-79}Rb$,$^{90-99}Rb$), cesium ($^{117-124,126}Cs$,$^{138,140-147}Cs$) and francium ($^{204-210,212}Fr$, $^{224-228}Fr$) were measured [70, 71, 72, 73]. To maintain a precision of $\sim$100 keV for the heavier nuclei a double focusing mass spectrometer with a mass resolution of R=5000 was acquired [70, 71]. The radioactive alkali isotopes were delivered by the ISOLDE on-line

mass separator. One of the advantages of this method is its rapidity, which beyond the source release times is limited only by the flight time through the spectrometer, thus allowing the measurement of nuclei with very short life times. A precision of 2×10^{-7} was typically obtained in the measurements.

The success of these direct mass measurements stimulated the interest of other groups including the now defunct programme at the on-line mass separator at TASCC-Chalk River [74]. In this case fusion-evaportaion reactions were employed to produce neutron deficient nuclei and a FEBIAD (forced electron beam arc discharge) type ion source was coupled to the spectrometer. Perhaps the most interesting feature of this programme was the detection of the characteristic gamma-rays of the nucleus of interest at the focal plane of the spectrometer. By varying the accerating voltage and hence stepping the beam across the exit slit, the beam profile could be precisely measured without any isobaric contamination. As a result precisions of 2×10^{-6} were reached for proton-rich isotopes of indium and bromine in the vicinity of ^{100}Sn [75].

Conventional mass spectrometers and on-line mass separators have provided a valuable contribution to the field. Their precision is, however, intrinsically limited by the precision attainable in the determination of the accelerating potential ($\sim 10^{-7}$). The desire for improved precision has driven the development of new techniques. As descibed below, these are in general based on frequency measurements.

b Radio Frequency Mass Spectrometers (RFMS)

In an RFMS the masses M_A and M_B are compared through their cyclotron frequencies ω_A and ω_B in the same homogeneous, static, magnetic field. If the two ions follow identical trajectories the frequencies and masses are related simply as,

$$\omega_A M_A = \omega_B M_B \tag{8}$$

A high resolution RFMS spectrometer MISTRAL[5] dedicated to the measurement of masses of short lived radioactive nuclei is currently in operation at ISOLDE, CERN [76]. The very short ($\sim$50 μsec) transit times makes this spectrometer a complementary tool to the high precision traps also in operation at ISOLDE.

The principle features of MISTRAL are a magnet exhibiting a highly homogeneous field, an RF-modulator and two symmetrical beam lines for the injection and extraction of the beam (figure 5). The low energy ($\sim$100 keV) beam furnished by the ISOLDE sources is injected into the spectrometer, executes two helical orbits and is then ejected. Whilst circulating within the spectrometer the ion crosses the RF-modulator at the first and third half-turns. The modulation frequency is adjusted so that the effect of the first passage through the RF field is cancelled by the second passage. As a result the kinetic energy of the ion remains unchanged. This occurs if the system is tuned such that,

$$\frac{\omega}{\omega_c} = n + 1/2 \tag{9}$$

[5]**Mass Measurements at ISOLDE with a Transmission RAdiofrequency spectrometer on-Line.**

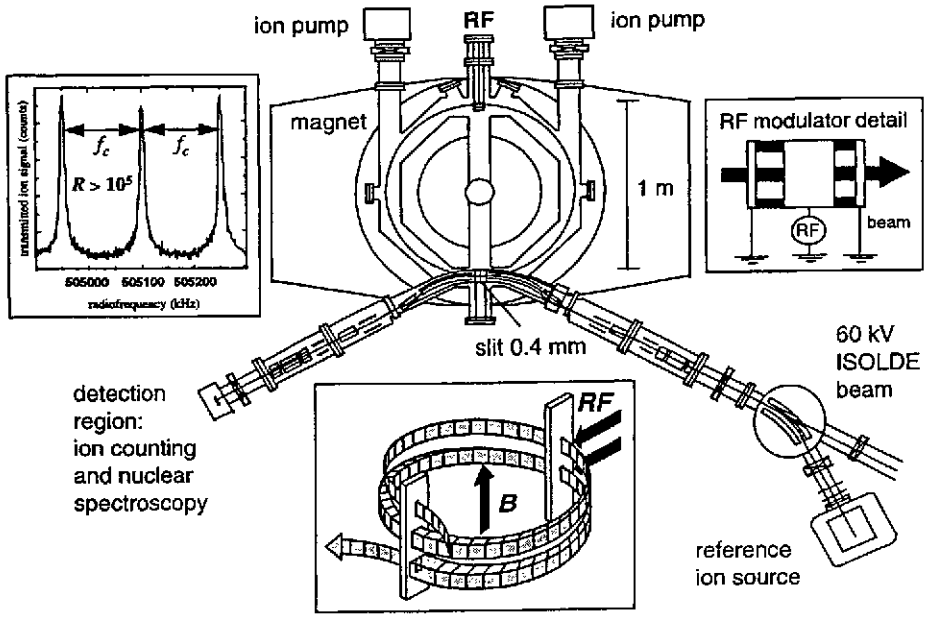

Figure 5: Overview of the MISTRAL radio frequency spectrometer [76].

where n are integers, ω is the frequency of the modulator and ω_c is the cyclotron frequency. When the frequency of the modulator is scanned, narrow peaks corresponding to the transmission maximums are observed in the intensity of the extracted beam for integer values of $\omega/\omega_c - 1/2$.

The first measurements of short-lived nuclei using MISTRAL have concentrated on the neutron-rich Ne, Na, Mg and Al isotopes in the vicinity of N=20 (section I) [77]. As displayed in figure 6, the precisions of the mass determinations in this region will be improved by nearly one order of magnitude over the earlier direct time-of-flight [3, 4], mass spectrometry [1] and decay [2] measurements.

c Ion traps as high precision mass spectrometers

The confinement of very low energy charged particles within static magnetic and electric fields – Penning trap – or time varying electric fields – Paul trap – represents a powerful tool for the manipulation of electrons, protons, ions and molecules [78]. Indeed, Penning traps have been employed for high precision mass spectrometry of many light stable particles. For example, the mass differences of the electron and positron [79], proton and antiproton [80, 81], helium-3 and tritium ions [82] and light stable atoms [83] have been measured with the highest accuracy achieved to date ($\sim 10^{-10}$). The basic principle of these measurements is the determination of the cyclotron frequency of the stored charged particle. The attainment of such high precisions owes much to developments in ultrahigh vacuum and superconducting magnet technology. In most of the experiments cited above the particles

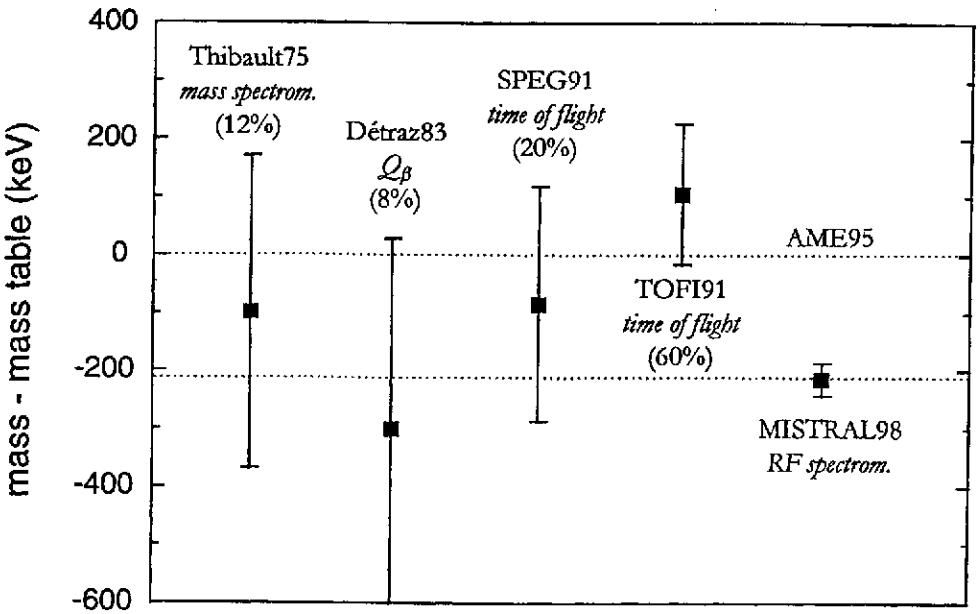

Figure 6: Comparison of earlier mass measurements for ^{30}Na and that recently furnished by the MISTRAL collaboration [86, 77].

of interest were created within the trap. As outlined below, one of the important facets in the use of traps with radioactive ions is the beam preparation and injection. In particular, the beams must be slowed down, bunched and isobars eliminated.

At present the only operating trap based system for the measurement of masses far from stability is ISOLTRAP at ISOLDE, CERN [84, 85, 86]. As the reader will no doubt glean from the references cited here, the high precesion mass determinations possible with even relatively short lived nuclei represent a significant advance in the exploration of the nuclear mass surface far from stability.

In the currently operating version of ISOLTRAP [86], the bunching and cooling needed for injection of the ions into the high precision measurement trap are performed using two smaller traps. The first trap consists of a gas-filled radiofrequency quadropole (RFQ) in which the continuous 60 keV ion beam delivered by the ISOLDE sources is captured and bunched[6]. The bunched ions are then injected into a larger cylindrical Penning trap which operates as a mass selective cooler. Typical mass resolving powers of R$\approx 10^5$ are achieved, which is sufficent to eliminate most isobaric contamination even relatively near stability. The ability to perform such purification is particularly important as the presence of unwanted ion species in the precision trap can lead to systematic errors such as those arising from the Coulomb interaction between different ions.

[6]In earlier versions the functions of this trap were performed through the collection of the ions on the foil of a secondary ion source, the heating of which produced very low energy ions via surface ionisation. Such a system, however, limited considerably the range of elements accessible to measurement and the overall efficiency.

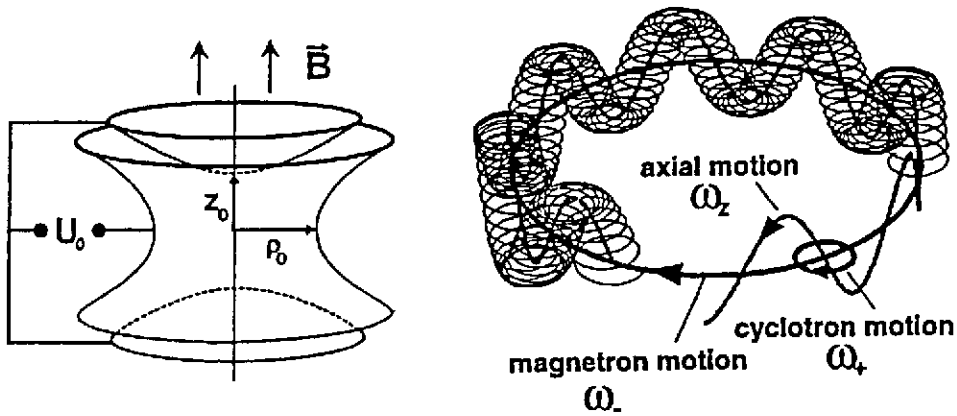

Figure 7: Schematic representation of a Penning trap and the trajectory of the trapped ions [78].

The final "precision" trap in which the mass measurements are carried out is a Penning trap. Here a homogeneous static magnetic field is used for the radial confinement of the ions and an axially symmetric static electric quadrupole field prevents the ions from escaping along the magnetic field lines (figure 7). In the absence of the electric field in-plane cyclotron motion around the Z-axis, with frequency $\omega_c = (q/m)B$ would occur. Similarly, in the absence of the magnetic field simple axial harmonic oscillations with frequency $\omega_z = 1/Z_o\sqrt{V_o(q/m)}$ would occur. As the electric quadrupole field has a repulsive in-plane component, the superposition of the magnetic dipole and the electric quadrupole fields produces cyclotron motion with a modified frequency ω_+ and a slow precession of this circular motion around the trap axis (magnetron motion) with frequency ω_-. This motion is combined with a simple axial harmonic oscillation of frequency ω_z (figure 7). The sum of ω_+ and ω_- is the cyclotron frequency ω_c. More explicitly,

$$\omega_\pm = \omega_c/2 \pm \sqrt{(\omega_c/2)^2 - \omega_z^2/2} \tag{10}$$

In order to measure the mass of a trapped nucleus an azimuthal quadrupole RF field ω_{rf} is applied. When resonance is achieved $\omega_{rf} = \omega_c = (q/m).B$ and the energy gain is a maximum. The degree of gain in energy is also a function of the time over which the RF field is applied. The increase in energy at resonance is detected by the measurement of the time-of-flight of the ions following ejection from the trap – ions in resonance with the applied RF field have the largest energy gain and thus reach the external ion detector faster than those off resonance (figure 8). The gain in kinetic energy for an ion with mass A=100 is of the order of 20 eV and the corresponding reduction in the flight time is of the order of 40%. The system is calibrated for the measurement of unknown masses using stable ions, such as ^{85}Rb and ^{133}Cs, produced using an internal ion source.

The first results obtained with ISOLTRAP were determinations of the mass excesses

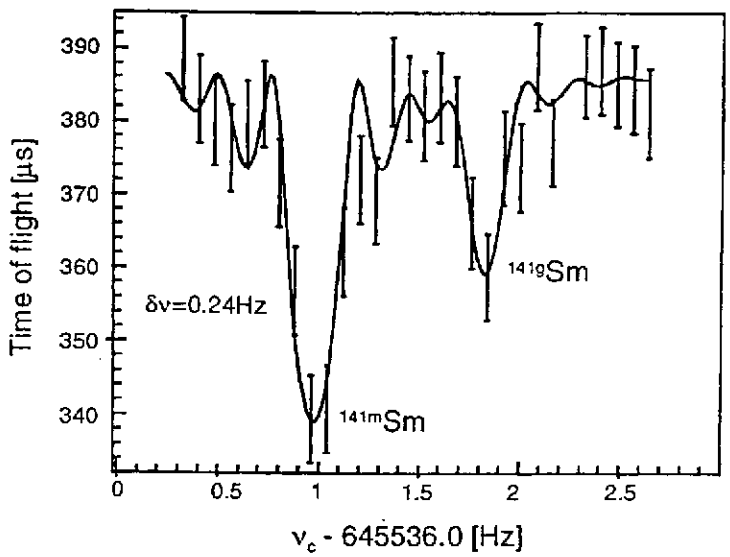

Figure 8: Resolved isomer and ground state in ^{141}Sm (ΔE=175 keV) [86].

of the cesium isotopes $^{118-137}Cs$ [87]. A resolving power of the order of 10^6 and a precision of 1.4×10^{-7} (~20 keV) were obtained. The ground and isomeric states of a nucleus have also been resolved for the first time in direct mass spectrometry demonstrating the power of the technique [88] – a mass resolution of some 70 keV was achieved for $^{78}Rb^{m,g}$ and $^{84}Rb^{m,g}$.

More recently an extensive programme of mass measurements of neutron deficient rare-earth isotopes in the mass 150 region has been completed [89]. Mass determinations with typical uncetainties of some 10-20 keV were reported for more than 40 isotopes of Pr, Nd, Pm, Sm, Eu, Dy and Ho, with halflives as low as ten seconds[7]. Current developments are centred around the use of the RFQ buncher trap, with preliminary results being obtained for neutron deficient Hg isotopes [86]. The refinement of the use of this trap should lead to increased efficiences and consequently a reduction in the halflives of the ions that can be measured.

3 Direct measurements at Intermediate and High Energies

a Time-of-Flight Methods

One of the most important advances in the last decade in the measurement of masses far from stability has been the development of direct time-of-flight techniques. The power of these approaches has arisen from the coupling of projectile fragmentation and target spallation/fragmentation reactions as production methods to high resolution spectrometers — SPEG at GANIL [90] and TOFI at Los Alamos [91]. Importantly, the very broad elemental and isotopic distributions resulting from such reactions combined with fast in-flight electromagnetic selection [16] can provide for the mapping of an entire region of

[7]These measurements still employed the secondary surface-ionisation source.

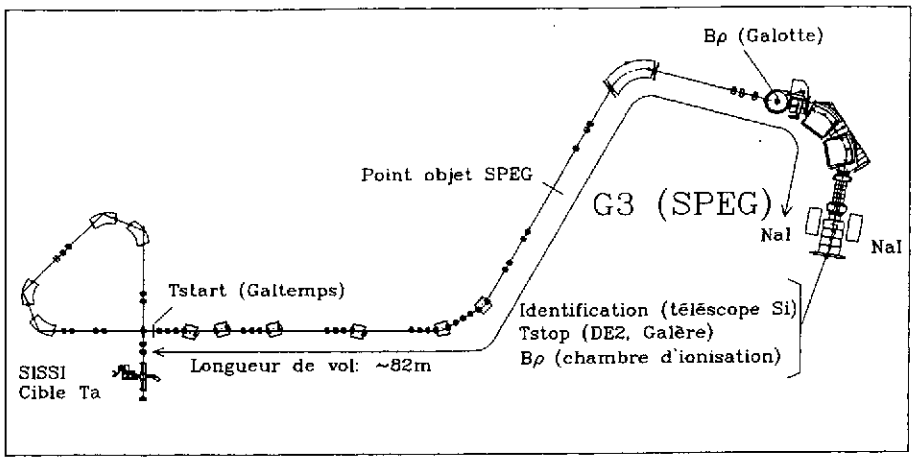

Figure 9: Overview of the SPEG direct time-of-flight mass measurement setup [100].

the nuclear mass surface in a single measurement, as shown, for example, in a recently completed investigation of neutron-rich nuclei in the region of the N=20 and 28 shell closures [100]. The experiments undertaken by both the TOFI and SPEG groups have provided a systematic survey of the nuclear mass surface for the neutron-rich nuclei from ^{11}Li to ^{72}Ni[92, 93, 92, 94, 3, 100, 4, 95, 96].

The direct time-of-flight technique requires in principle (equation 6) only the determination, for a particular rigidity, of the velocity of the ion. In the case of the now discontinued programme based on the TOFI (Time-of-Flight Isochronous) recoil spectrometer [94, 93, 4, 95, 96], the high current (1 mA) 800 MeV proton beam from LAMPF was used to produce neutron-rich nuclei via the spallation and fission of a thin ^{nat}Th target. A small fraction of the products emitted at low energy (~2-3 MeV/nucleon) were captured using a secondary transport line, which incorporated a mass-to-charge filter to reject the intense near stable species, and transmitted to TOFI. The TOFI spectrometer was a highly symmetrical system consisting of four identical dipole elements arranged such that the flight time of ions of a particular m/q traversing the system was independent of the velocity. The measurement of the time-of-flight (TOF) of the ions traversing the 14 m flight-path of TOFI was made using secondary electron, fast timing detectors, comprising of thin foils coupled to microchannel plates [97]. A timing resolution (FWHM) of some 200 ps was usually obtained, corresponding, for a typical flight time of ~600 ns, to a mass-to-charge resolution of $\sim 3\times10^{-4}$.

In the case of the programme based around the SPEG spectrometer [92, 3, 98, 99, 100], projectile fragmentation of high intensity ($\sim10^{11-12}$ pps), intermediate energy (~50-70 MeV/nucleon) heavy-ion beams (^{40}Ar, ^{48}Ca, ^{78}Kr) from the GANIL coupled cyclotrons have been used to produce the nuclei of interest. The projectile-like fragments emitted from the production target, located at the exit of the second cyclotron, are selected using the beam analysis spectrometer and transported along a doubly achromatically tuned beam line to the focal plane of SPEG, a flight path of 82 m (figure 9). The TOF measurement

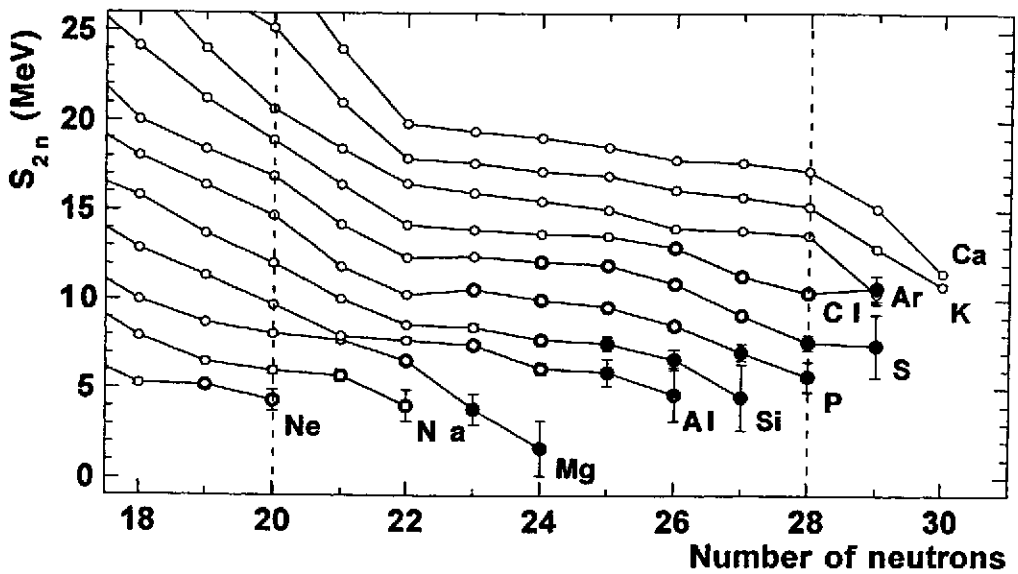

Figure 10: Two-neutron separation energies in the region of the N=20 and 28 shell closures [100].

is made, as in the TOFI experiments, using a pair of microchannel plate detectors — flight times are typically of the order of 1 μs. The magnetic rigidity of each ion is derived from a position measurement made using a thin position sensitive parallel plate avalanche counter or microchannel plate detector system located at the dispersive image plane of SPEG. Resolutions (FWHM) of $\sim 10^{-4}$ in the rigidity and $\sim 2.5 \times 10^{-4}$ in the flight time are typically achieved, corresponding to a mass resolutions of $\sim 3 \times 10^{-4}$.

In both the TOFI and SPEG measurements a large number of nuclei ($\sim$100) are transmitted in any one setting of the beam line and spectrometer. The nuclei of known masses are used to provide a calibration from which the unknown masses are derived. Such a large number of reference masses over a wide range of Z and A is particularly important in providing final mass determinations with precisions of the order of 10^{-6} [101]. The final uncertainties range from $\sim$100 keV for nuclei relatively close to stability (many thousands of events) to $\sim$1MeV for those approaching the ends of isotopic chains (some tens of events).

The most recent measurements of this type are those undertaken by Sarazin *et al.* using the SPEG spectrometer in conjunction with a high intensity ^{48}Ca beam and the SISSI device for increased efficiency in the collection of the reaction products [100]. The masses of some 30 neutron-rich nuclei in the mass range A=29-47 were measured (figure 10), providing evidence for changes in shell structure around N=28 for the neutron-rich isotopes of Cl, S and P.

A number of caveats must be noted regarding the accuracy of direct time-of-flight measurements. Firstly, the population of isomeric states with lifetimes of the order of the flight time through the system ($\sim 1\mu$s) presents a potential problem, as the resolution of the TOFI and SPEG systems are not sufficient to resolve the typical mass difference between

the ground and excited states. Measurements of such mixed states will lead to a less bound mass determination, as has been observed for ^{32}Al [92], ^{68}Ni [96] and ^{43}S [100]. Clearly, well known nuclei with isomeric states must be excluded from the calibration.

In the case of the TOFI measurements, undertaken at low secondary beam energies, care needed to be taken to avoid isobaric contamination, which may arise from the limited resolution in the determination of the atomic number. Such effects would appear to have biased the earliest measurements of the masses of ^{27}Ne and ^{30}Na [94] and in practice limit the TOFI based programme to the heaviest systems so far measured [96]. Similarly, the problems associated with charge states other than Q=Z for heavy systems, complicate the SPEG based measurements [99]. Given the presently attainable resolutions, the limit for obtaining reasonable mass determinations would appear to be A$\sim$80.

In order to extend the method of time-of-flight measurement to heavier nuclei and to achieve higher precision for the lighter ones, a substantially longer flight-path is required. Given the physical limitations on a rectilinear flight path, this can best be achieved if the ions follow a spiral or circular path. These considerations have motivated new techniques which use time-of-flight or frequency measurements associated with circulating beams.

b Storage Rings

Novel cyclic methods have recently been developed at GSI for the measurement of the masses of nuclei far from stability produced as the products of the projectile fragmentation of heavy relativistic beams [102]. The the nuclei of interest are stored in the Experimental Storage Ring (ESR) [103], where the revolution frequencies are measured.

The fully ionised secondary ions at GSI are produced by projectile fragmentation of the relativistic primary beams provided by the SIS heavy-ion synchrotron, which can furnish ions of all elements up to Uranium with energies up to some 1 to 2 GeV/nucleon. The reaction products are separated in-flight with the FRS Fragment Separator [104] using standard magnetic rigidity and energy loss analyses [16]. The secondary beams are subsequently injected and accumulated in the ESR. The ESR was designed to accumulate, store and cool heavy ions with energies up to 500 MeV/nucleon [102]. The cooling is achieved through the Coulomb interaction of the circulating ions with "cold" electrons.

The ESR can be used in two different modes to measure the mass-to-charge ratios of the circulating ions. Each method is based on the principle that for a particle with rest mass m and velocity v, circulating in a ring with a revolution time T, the resolution $(\Delta m/q)/(m/q)$ is related to the time resolution $\Delta T/T$ and the velocity spread Δv as,

$$\frac{\Delta m/q}{m/q} = \gamma_{tr}^2 \frac{\Delta T}{T} + (\gamma_{tr}^2 - \gamma^2)\frac{\Delta v}{v} + \gamma_{tr}^2 \frac{\Delta B}{B} \tag{11}$$

where γ is the relativistic factor and $\gamma_{tr} = \sqrt{1 - v_{tr}^2/c^2}$ is the value at the so-called transition energy which is a constant inherent of the ion-optical tuning of the ring[8]. $\Delta B/B$ is the relative magnetic field non-uniformity integrated over all paths within the ring. This term

[8]At the transition point the increase in velocity compensates for the increased flight path and the

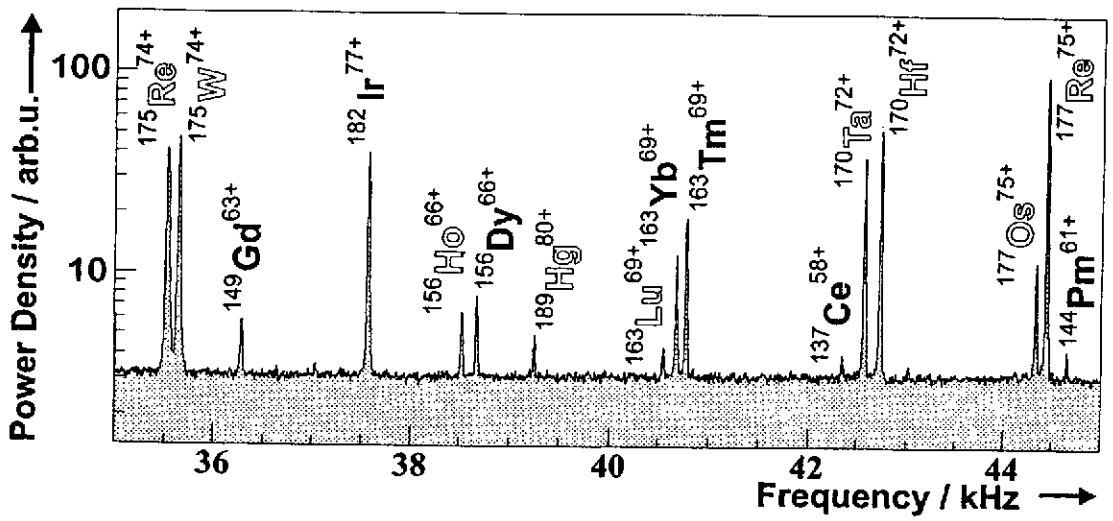

Figure 11: Example of the Schottky spectrum of stored and cooled fragments in the ESR [107]. Nuclei with known (reference) masses are noted in bold letters.

is usually small. The principle limitation on the mass resolution is the velocity dependent term.

In the first method developed, the mass resolution is improved by the reducing the velocity spread Δv via electron-cooling of the stored beam. If the beam is cooled and all ions have the same velocity, the frequency differences will depend only on m/q and the mass of the ion is thus directly related to the revolution frequency. The frequency is measured using the Schottky noise technique whereby a signal is induced by the circulating particles on metallic probes located within the ring [105]. In order to isolate the very small signals from thermal noise the frequency spectrum is generated by Fourier transformation. The frequency spectrum (see, for eample, figure 11) contains peaks at all harmonics of the circulation frequencies of the stored ions. High harmonics ($\sim$20) are choosen to provide the best signal to noise ratio.

The cooling times are typically at least 1 s and the method is thus restricted to the measurement of nuclides with comparable or longer halflives and which are produced with reasonably high yields. The pilot experiments demonstrated the feasibility of the techniques involved by storing and cooling a ^{18}F beam [106]. The mass was determined with a precision of 80 keV or 5×10^{-6}. In a spectacular demonstration of the method, the masses of over 100 heavy neutron-deficient nuclides in the Hf-Bi region produced by the fragmentation of a 930 MeV/nucleon ^{209}Bi beam were measured for the first time in a recent experiment [107]. Precisions of some 100-150 keV were obtained.

In the second of the methods [108, 109], which is still under development, the ESR is operated in an isochronous mode. In simple terms, the ion optics of the ring are tuned such

---

revolution frequency thus becomes velocity independent – that is, the ring operates in an isochronous mode.

that $\gamma = \gamma_{tr}$, thus eliminating the velocity dependent term in equation 11. In this case the ESR can be used as a time-of-flight mass spectrometer for very short lived exotic nuclei produced with low yields. For a single turn measurement, if the timing uncertainty of the detection system is around 150 ps, and the flight time is ~500 ns, the mass resolution is $\sim 3 \times 10^{-4}$. In multi-turn measurements ($N_T \geq 100$) an improved mass resolution may be achieved. Beyond several tens of turns, however, higher order aberrations can become significant and the optimum performance is expected for $N_T \approx 30$. Initial testing with stable beams has demonstrated the viability of the technique [109] and it is expected that the measurement of unknown masses will soon be performed.

IV Conclusions

The aforegoing discussion has only briefly touched on some of the techniques used to measure masses of nuclei far from stability. Due to restrictions in time and space only those techniques which have been or currently are being used routinely have been described[9]. As the more alert reader may have noted the use of cyclotrons as high resolution mass spectrometers [110], for example, has not been covered.

It is worthwhile reiterating, as discused in the accompanying course by Georges Audi, that mass measurements with a particular technique should not be taken in isolation. Moreover, the connections between different experiments are often of considerable importance. As an example, one may consider the mass differences derived from α-decay chains, which are often not linked to known masses. Careful measurement of the mass of a single member of such decay chains (figure 12) can provide a significant windfall which may extend further from stability than the measurement itself.

Precise mass determinations for nuclei less exotic than those at the frontier between known and unknown masses are, despite the lack of glamour, of considerable importance. In particular, these nuclei provide the reference masses for the calibration of measurements far from stability.

In the near future, the advent of new radioactive beam facilities can be expected to add new leases of life to the techniques outlined here. For example, transfer reactions may see a renaissance through the availability of intense secondary beams, whilst invariant mass measurements may be extended to heavier unbound systems. More generally, direct measurements will be able to be used to map the mass surface even further from stability. In doing so it is almost certain that new regions of interest in the nuclear landscape will be uncovered.

Acknowledgements

The written version of this lecture is based on the review article written in collaboration with Wolfi Mittig and Alinka Lépine-Szily [15]. My thanks are also due to Wolfi for letting

[9]Some degree of personal bias arising from my own experiences should also be admitted to.

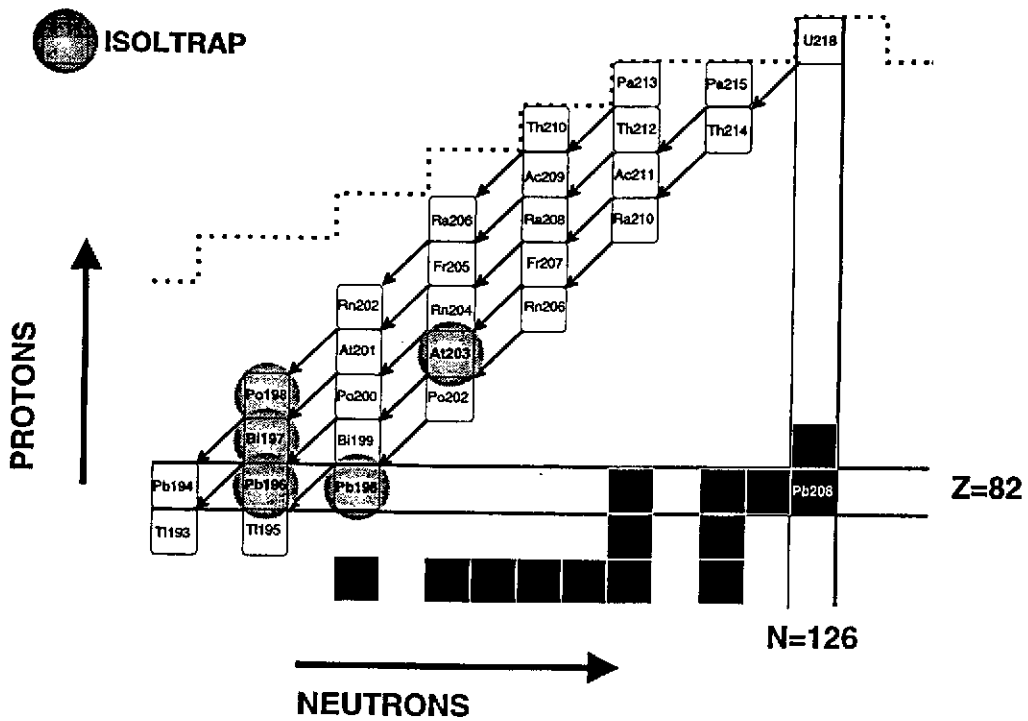

Figure 12: Connections provided by recent ISOLTRAP mass measurements to α-decay chains [86]. The dotted line indicates the borderline of known nuclei.

me experience the delights of life with the MODCOMP ("qui mange des huitres"). I am also grateful to Dave Lunney for supplying me with some of the material used here as well as introducing me to the wines of Givry.

Bibliography

[1] Thibault C et al, Phys. Rev. **C12**, 644 (1975).

[2] Détraz C, et al., Nucl. Phys. **A394**, 378 (1983).

[3] Orr NA, et al., Phys. Lett. **B258**, 29 (1991).

[4] Zhou XG, et al., Phys. Lett. **B260**, 285 (1991).

[5] Warburton EK, et al., Phys. Rev. **C41**, 1147 (1990)

[6] Poves A, Retemosa J, Nucl. Phys. **A571**, 221 (1994)

[7] Klotz G et al., Phys. Rev. **C47**, 2502 (1993)

[8] Motobayashi T et al., Phys. Lett. **B346**, 9 (1995); Pritychenko BV et al., **B461**, 322 (1999)

[9] R Neugart, A Wöhr, eds, *Proc. of the 6th Int. Conf. on Nuclei far from Stability and the 9th Int. Conf. on Atomic Masses and Fundamental Constants* (Institute of Physics Publishing, Bristol, 1993).

[10] M de Saint Simon, O Sorlin, eds, *Proc. of the Int. Conf. on Exotic Nuclei and Atomic Masses — ENAM95* (Editions Frontières, Gif-sur-Yvette, 1995).

[11] Sherrill BM, Morrissey DJ, Davids CN, eds, *Proc. ENAM98 — Exotic Nuclei and Atomic Masses* (AIP Conf. Proceedings vol. 455, AIP, Woodbury, New York, 1998)

[12] Lunney D, Audi G, Kluge HJ,ed, *Proc. of the 2nd Euroconference on Atomic Physics at Accelerators — APAC2000* (Kluwer Scientific, Dordrecht, The Netherlands, 2001)

[13] Audi G, Wapstra AH, Nucl. Phys. **A595**, 409 (1995)

[14] Audi G, Wapstra AH, Nucl. Phys. **A565**, 1 (1993)

[15] Mittig W, Lépine-Szily A, Orr NA, Ann. Rev. Nucl. Part. Sci. **47**, 27 (1997)

[16] Geissel H, Münzenberg G, Riisager K, Ann. Rev. Nucl. Part. Sci. **45**, 529 (1995)

[17] Mueller AC. Sherrill BM, Ann. Rev. Nucl. Part. Sci. **43**, 163 (1993)

[18] Cerny J, in *Proc. of the Third Int. Conf. on Nuclei far from Stability* (CERN 76-13, 1976), p 225

[19] Benenson W, in *Proc. of the Third Int. Conf. on Nuclei far from Stability* (CERN 76-13, 1976), p 235

[20] Thorn CE, et al., Phys. Rev. **C30**, 1442 (1984)

[21] Davis NJ, et al., Phys. Rev. **C32**, 713 (1985)

[22] Stokes RH, Young PG, Phys. Rev. **178**, 1789 (1969)

[23] Cerny J, et al., Phys. Rev. Lett **16**, 469 (1966)

[24] Benenson W, et al., Phys. Rev. **C9**, 2130 (1974)

[25] Woodward CJ, et al., Phys. Rev **C27**, 27 (1983)

[26] Kato S, et al., Phys. Rev. **C42**, 563 (1990); Phys. Rev. **C41**, 2004 1990); Phys. Rev. C41, 1276 (1990); Phys. Rev. **C39** 818 (1989)

[27] Stiliaris E, et al., Z. Phys. **A326**, 139 (1987)

[28] Mohar MF, et al., Phys. Rev. **C38**, 737 (1988)

[29] Woods CL, et al., Nucl. Phys. **A484**, 145 (1988)

[30] Mayer WA, et al., Z. Phys. **A319**, 287 (1984)

[31] Drumm PV, et al., Nucl. Phys. **A441**, 95 (1985).

[32] Woods PJ, et al., Phys. Lett. **B182**, 297 (1986); Z. Phys. **A321**, 119 (1985)

[33] Fifield LK, et al., Nuc. Phys. **A484**, 117 (1988); Nucl. Phys. **A453**, 497 (1986); Nucl. Phys. **A440**, 531 (1985)

[34] Young BM, et al., Phys. Rev. Lett. **71**, 4124 (1993)

[35] Bohlen HG, et al., Nucl. Phys. **A583**, 775 (1995)

[36] Wilcox KH, et al., Phys. Lett. **59B**, 142 (1975)

[37] Amelin AI, et al., Sov. J. Nucl. Phys. **52**, 501 (1990)

[38] Bohlen HG, et al., Z. Phys. **A344**, 381 (1993)

[39] Young BM, et al., Phys. Rev. **C49**, 279 (1994)

[40] Caggiano JA, et al., Phys. Rev. **C60**, 064322 (1999)

[41] Kryger RA, et al., Phys. Rev. **C47**, R2439 (1993)

[42] Thoennessen M, et al., Report MSUCL-1180, Oct. 2000; Phys. Rev. **C** ,in press

[43] Catford W, et al., Nucl. Phys. **A489**, 347 (1988)

[44] Catford W, et al., Nucl. Phys. **A503**, 263 (1989)

[45] Fifield LK, Orr NA, Nucl. Instr. Meth. Phys. Res. **A288**, 360 (1990)

[46] Nann H, et al., Phys. Lett. **96B**, 261 (1980)

[47] Burleson GR, et al., Phys. Rev. **C22**, 1180 (1980)

[48] Morris Cl, et al., Phys. Rev. **C25**, 3218 (1982)

[49] Gilman R, et al., Phys. Rev. **C30**, 958 (1984)

[50] Seth KK, et al., Phys. Rev.Lett. **58**, 1930 (1987); Phys. Lett **B173**, 397 (1986); Phys. Rev. Lett **41**, 1589 (1978)

[51] Kobayashi T, et al., Nucl. Phys. **A538**, 343c (1992)

[52] Hansen PG, Jensen AS, Jonson B, Ann. Rev. Nucl. Part. Sci. **45**, 591 (1995)

[53] Bohlen HG, et al., Z. Phys. **A330**, 227 (1988)

[54] Ostrowski AN, et al., Phys. Lett. **B338**, 13 (1994)

[55] Ostrowski AN, et al., Z. Phys. **A343**, 489 (1992)

[56] Kalpakchieva R, et al., Eur. Phys. J. **A7** , 451 (2000)

[57] Korsheninnikov AA, et al., Phys. Lett. **B326**, 31 (1994)

[58] Kryger RA, et al., Phys. Rev. Lett. **74**, 860 (1995)

[59] Goosman DR, Alburger DE, Phys. Rev. **C10**, 756 (1974)

[60] Decker R, et al., Nucl. Instr. Meth. Phys. Res. **A192**, 261 (1982)

[61] Bom VR, Nucl. Instr. Meth. Phys. Res. **A207**, 395 (1983)

[62] Gross M, et al., Nucl. Instr. Meth. Phys. Res. **A311**, 512 (1992)

[63] Przewloka M, et al., Z. Phys. **A342**, 23 (1992), Z. Phys. **A342**, 27 (1992)

[64] Parks LA, et al., Phys. Rev. **C15**, 730 (1977)

[65] see, for example, Enge H *Introduction to Nuclear Physics* (Addison-Wesley, 1966)

[66] Keller H, et al., Nucl. Instr. Meth. Phys. Res. **A300**, 67 (1991); Z. Phys. **A340**, 363 (1991)

[67] Plochocki A, et al. , Nucl. Phys. **A332**, 29 (1979)

[68] Roeckl E, Rep. Progr. Phys. **55**, 1661 (1992)

[69] Gross M, et al. , in Ref. [1], p 77

[70] Epherre M, et al., Phys. Rev. **C19**, 1504 (1979)

[71] Epherre M, et al., Nucl. Phys. **A340**, 1 (1980)

[72] Audi G, et al., Nucl. Phys. **A378**, 443 (1982)

[73] G.Audi, et al., Nucl.Phys. **A449**, 491 (1986)

[74] Schmeing H, et al., Nucl. Instr. Meth. **186**, 47 (1981)

[75] Sharma KS, et al., Phys. Rev. **C44**, 2439 (1991)

[76] Lunney MD, et al. Hyperfine Interactions **99**, 105 (1996)

[77] Lunney MD, et al. in ref [12]; Audi G et al, in preparation; Toader C, Thèse, Universite Paris XI (1999); Monsanglant C, Thèse, Universite Paris XI (1999)

[78] Lunney D, *Ecole Internationale Joliot-Curie de Physqiue Nucléaire, 1999*, p 85

[79] Schwinberg PB, Van Dyck RS, Dehmelt HG, Phys. Lett. **A81**, 119 (1981)

[80] Gabrielse G, et al., Phys. Rev. Lett. **74**, 3544 (1995)

[81] Phillips D, et al., Physica Scripta **59**, 307 (1995)

[82] Van Dyck RS, Farnham RL, Schwinberg PB, Phys. Rev. Lett. **70**, 2888 (1993)

[83] DiFilippo F, et al., Phys. Scrip. **59**, 144 (1995); Phys. Rev. Lett. **73**, 1481 (1994)

[84] Kluge HJ, Bollen G, Nucl. Instr. Meth. Phys. Res. **B70**, 473 (1992)

[85] Kluge HJ, in Ref. [2], p 3

[86] Lunney MD, Bollen G, Hyperfine Interactions **129**, 149 (2000)

[87] Stolzenberg H, et al., Phys. Rev. Lett. **65**, 3104 (1990)

[88] Bollen G, et al., Phys. Rev. **C46**, 2140 (1992)

[89] Beck D, et al., Eur. Phys. J. **A8**, 307 (2000)

[90] Bianchi L, et al., Nucl. Instr. Meth. Phys. Res. **A276**, 509 (1989)

[91] Wouters JM, et al., Nucl. Instr. Meth. Phys. Res. **A240**, 77 (1985); Nucl. Instr. Meth. Phys. Res. **B26**, 286 (1987)

[92] Gillibert A, et al., Phys. Lett. **B192**, 39 (1987)

[93] Wouters JM, et al., Z. Phys. **A331**, 229 (1988)

[94] Vieira DJ, et al., Phys. Rev. Lett. **57**, 3253 (1986)

[95] Tu XL, et al., Z. Phys. **A337**, 361 (1990)

[96] Seifert HL, et al., Z. Phys. **A349**, 25 (1994)

[97] Kraus RH, et al., Nucl. Instr. Meth. Phys. Res. **B26**, 280 (1987).

[98] Gillibert A, et al., Phys. Lett. **B176**, 317 (1986)

[99] Chartier M, et al., Nucl. Phys. **A637**, 3 (1998)

[100] Sarazin F, et al., Phys. Rev. Lett. **84**, 5062 (2000); Thèse Université de Caen (1999)

[101] Mittig W, in *Proc. Int. Symposium on Structure and Reactions of Unstable Nuclei, ed K Ikeda, Y Suzuki* (World Scientific, Singapore, 1991), p 8

[102] Klepper O, et al., Nucl. Instr. Meth. Phys. Res. **B70**, 427 (1992)

[103] Franzke B, Nucl. Instr. Meth. Phys. Res. **B24/25**, 18 (1987)

[104] Geissel H, et al., Nucl. Instr. Meth. Phys. Res. **B70**, 286 (1992)

[105] Franzke B, et al., Phys. Scrip. **59**, 176 (1995)

[106] Geissel H, et al., Phys. Rev. Lett. **68**, 3412 (1992)

[107] Radon T et al., Nucl. Phys. **A677**, 75 (2000)

[108] Wollnik H, Nucl. Instr. Meth. Phys. Res. **B26**, 267 (1987)

[109] Haussmann M, et al., Nucl. Instr. Meth. Phys. Res. **A446**, 569 (2000)

[110] Auger G, et al., Nucl. Instr. Meth.Phys. Res. **A350**, 235 (1994); Chartier M, et al., Phys. Rev. Lett. **77**, 2400 (1996)